Journal of Solid Mechanics Vol. 13, No. 1 (2021) pp. 54-67
DOI: 10.22034/jsm.2020.1885686.1528

Experimental and Numerical Investigation on Geometric Parameters of Aluminum Patches for Repairing Cracked Parts by Diffusion Method

S. Dehghanpour [1], A.R. Nezamabadi [1,*], M.M. Attar [2], F. Barati [2], M.Tajdari [3]

[1] *Department of Mechanical Engineering, Islamic Azad University, Arak Branch, Arak, Iran*
[2] *Department of Mechanical Engineering, Hamedan Branch, Islamic Azad University, Hamedan, Iran*
[3] *Department of Mechanical Engineering, Faculty of Electrical, Mechanical and Computer Engineering, University of Eyvanekey, Eyvanekey, Iran*

Received 23 September 2020; accepted 10 December 2020

ABSTRACT

Repairing cracked aerial structures using patches is a common way to restore mechanical properties, strength and extend fatigue life. The performance of such patches can be obtained by comparing the maximum amount of force tolerated by the repaired piece with the unrepaired piece. The shape and dimensions of the patch used to repair the crack and the way the patch is bonded affect the repair quality which are of great importance. Therefore, in this paper, we investigate the factors affecting the diffusion bonding between the patch and the piece. The impact of the shape of the aluminum patch attached on a 10 mm central crack piece and perpendicular to the loading direction (mode I) is studied experimentally and numerically. The optimum conditions for the diffusion connection including the pressure, time and temperature of the connection were obtained experimentally using a composite rotatable centered design and in the connection made under these conditions, the patch shape and aspect ratio was considered as variables of design, and the results were obtained for square, rectangular, circular and elliptical patches. At the end, it was found that the best connection under the pressure conditions of 570 °*C*, 70 *bar* and 100 min was formed and the rectangular patch efficiency was greater whereas its extent is more in line with crack than the other modes. At a fixed area, the different patch geometries investigated in this study were able to influence up to 80% of the maximum force tolerated by the repaired parts. In addition, there is an acceptable convergence between experimental and numerical results.

Keywords: Crack repair; Diffusion bonding; Bonding temperature; Aluminum patch; Optimum patch design.

1 INTRODUCTION

DAMAGE during the life of space frames is a natural property, which is inevitable. Cracks can become

*Corresponding author. Tel.: +98 9181615153.
E-mail address: a-nezamabadi@iau-arak.ac.ir (A.R.Nezamabadi)

apparent due to inherent faults and holes, stress concentration factors, welding, static, dynamic and alternative loading, or spontaneous growth. Strategies for dealing with cracked pieces in various industries such as aerospace, automotive, marine and military are as replacement and restoration of the defective part. Since the replacement of the cracked block is not always possible due to factors such as time, cost and difficulty, the repair of parts can be a practical and logical solution [1]. The main purpose of repair is to restore the strength and stiffness of the structure to before defective appearance conditions. Parts can be repaired in two ways, mechanical repair by screw or rivet and glue repair by gluing the composite to the breakdown site. Mechanical restoration has been the subject of much attention in the past and is less used today because of the hole in the repair process, thereby increasing stress concentration points and the potential for damage to hydraulic and electrical systems and the impossibility of second and subsequent repairs. The latter method, which is widely used in the aviation and other industries, focuses on new stresses not imposed on the structure and has many advantages, including moisture insulation, surface integrity and adhesion, surface roughness and low weight, which has the least impact on airflow for aerodynamically important components, it is possible to have favorable mechanical properties such as high strength to weight ratio, flexibility in type design, weight percentage and fiber layout and also it is easily applied on curved surfaces[2]. Baker, as one of the pioneers of this type of restoration, has mentioned in his study the wide range of benefits of repairing metal parts with composite patches [3]. Restoration of cracked parts by the use of paste-based composite patches also has some disadvantages. The major disadvantage of such patches is the adhesive used during the repair process and in many cases before the load is transferred to the patch the shear stress in the adhesive reaches its maximum value and separates the patch from the part and the patch actually loses its performance. In addition, the linear expansion coefficient of these composites is lower than that of the metals and the temperature changes occurring at different altitudes of the aircraft causes thermal stress and eventually patch separation [4, 5]. In addition, thermal instability, thermal and electrical insulation, flammability and structural integrity are other disadvantages of this method. It seems necessary to introduce a patch and connection method that, while having advantages, partially removes the mentioned flaws. In this study, an aluminum alloy patch with a different final strength from the cracked part and a permanent diffusion joint were used to attach the patch to the cracked part. Diffusion bonding is a very useful and valuable technique for coupling components, especially in the aerospace industry, and involves pressing the heated components to connect the surface atoms of the components as a metal-to-metal bond [6]. In this method, parameters such as the pressure, temperature, holding time and the surface roughness of the specimens play a fundamental role in determining the bonding strength and can be precisely adjusted the temperature, pressure and time hence control the formation of intermetallic compounds[7-10]. In addition to the patch type and how it is bonded, geometrical parameters such as thickness, dimensions and shape of the patch also affect repair efficiency. Mahadesh Kumar and Hakeem studied the optimally symmetric patch shape for repair of central cracked thin sheet in the I mode numerically and investigated the amount of SIF reduction coefficient in circular, elliptical and rectangular patches [11]. Brighenti presented the optimal design method with genetic algorithm for repair and showed that patch shape greatly influences the failure and fatigue life of components repaired with duplex patch [12]. Chukwujekwu Okafor et al applied an extended finite element model to analyze the stress distribution in a single-sided repaired octagonal patch and examined the details of the stress distribution in the cracked part, patch and glue [13]. Albedah et al. estimated the stress intensity factor by using finite element analysis, in one-side and two-side circular patch repair and compared the patch-to-weight efficiency ratio in these two modes [14]. Most of the studies on patch shape are numerical and no major empirical studies have been performed on patch shape.

In this study, the efficiency of square, rectangular, circular and elliptical patches has been studied experimentally and numerically. Although many studies have been done on mechanical engineering on crack repair, the problems with this method are still persistent, and further studies are needed on how to patch the part and the optimal shape of the patch. The innovation of the present study is to select a homogeneous patch with more elastic modulus with damaged piece and without adhesive bonding using diffusion process and the selection of geometrical parameters compatible with this type of bonding.

2 METHODS AND MATERIAL

2.1 Diffusion process

In the present study, an innovation has been provided for the fusion of patches made of aluminum and its alloys for the repair of cracked aluminum fragments by diffusion method. The process involves performing a chemical step on the surface of the components and a surface abrasion mechanical operation to remove the aluminum oxide layer and eventually squeeze the piece and patch it over heat and over time to form a diffusion bond. The present study is concerned with the diffusion bonding technique of cracked aluminum patch and its alloys as a composite structure.

Aluminum and most of its alloys have a rigid, sticky surface of oxide, which prevents diffusive bonding. Due to its favorable physical properties, aluminum, with low density and high strength, is an ideal metal for use in various industries, particularly in the aerospace industry but the inability of composite molding and fabrication in conventional ways has led to design limitations.

Surface oxide on aluminum is formed rapidly even at relatively low oxygen pressures, and it is not easily possible to remove the oxide layer and create an oxide-free surface for diffusion bonding and the interval between the end of the surface preparation and the diffusion bonding process is very important and parts shouldn't be in the air for more than about twenty minutes and eventually one hour. The components have been partially deoxidized after the wear operation using various acids, and the experiments have shown that the above chemical process is effective in completely eliminating the oxide layer. Only the parts that are subjected to diffusion are oxidized, and the entire surface of the fragment is not to be oxidized.

In this process, the three parameters of temperature, pressure and time are important and affect each other. The most important factor in this process is temperature, because important and influential phenomena in the penetration joint such as creep are very temperature sensitive [15]. Increasing the temperature of the intrusive heat treatment increases the volume of interaction between the atoms of the coating layer and the base metal, so that lowering the process temperature eliminates the penetration zone in the joint layer of the bonding layers. The bonding temperature in this method is between 60 and 95% of the melting temperature of the base metal. Research has shown that higher temperatures make it difficult for atoms to penetrate the joint and cause deformation of the contact surface [16]. Pressure is also an important factor and its main role is in the intrusive bonding process of breaking the oxide layers formed on the metal surface [15]. The pressure applied in this process in various studies is usually in the range of 0.1 to 20 *Mpa* [17]. Diffusion bonding is a time-consuming process that decreases bonding time with the increasing temperature. The process time and the holding time of the component at the desired temperature should be sufficient to allow the optimum permeability, But too much time and excessive holding at this temperature also reduces the physical, chemical and mechanical properties [18]. The device designed to make the diffusion bonding and its schematic shape are shown in Figs. 1 and 2 respectively. Fig. 3 illustrates the different stages of diffusion process. In the first stage, the initial asperity contact between the surface roughnesses is formed. In the second stage, the deformation occurs and the interfacial boundary is formed, in the third stage the grain boundary migration begins and the cavities begin to be removed, and in the fourth stage the volumetric penetration is made and the cavities are removed.

Fig.1
Device designed to create diffusion bonding.

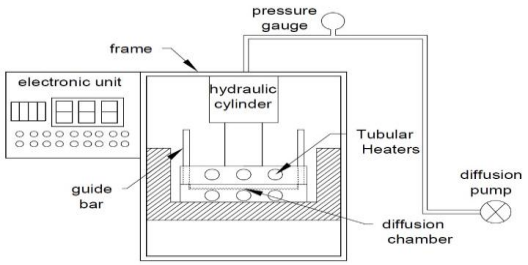

Fig.2
Schematic design of diffusion device.

2.2 Design of experiment

To obtain the experimental shear bond strength created by diffusion, rectangular specimens of 120*mm* × 50*mm* were cut from 1*mm* thick sheets of Al 6061 and Al 7075 alloy according to Fig. 4. Chemical analysis of the raw materials is given in Table 1. The surface oxide was then extracted by sic paper with 1000 grit and washed in acetone solution and then immersed in Naoh solution (8*g* / *lit*) for 2 minutes and in HNO3 solution(15% vol) for 5 minutes were neutralized at room temperature and finally washed with ultrasonic machine in acetone and cleaned [19].

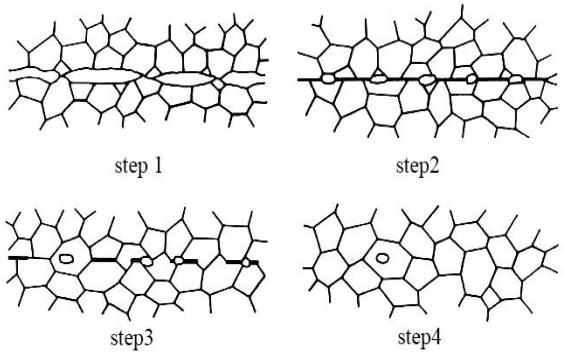

Fig.3
Different stages of diffusion process.

After the above mechanical and chemical steps, the components are placed in a diffusion system designed according to Fig. 2, and according to previous references [20-22] independently controllable parameters affecting the quality of diffusion connection are three temperature, pressure and time of bond formation was determined according to Table 2. Due to wider range of working limits of process parameters, a three-factor, five-level and central composite rotatable centered design was selected to manage the tests, as showed in Table 3.

The samples were cooled inside the furnace under a protective atmosphere at a temperature reduction rate of about 5 ° *C* / *min* [23]. The diagram of the junction time cycle of the samples tested for 120 minutes is shown in Fig. 5.

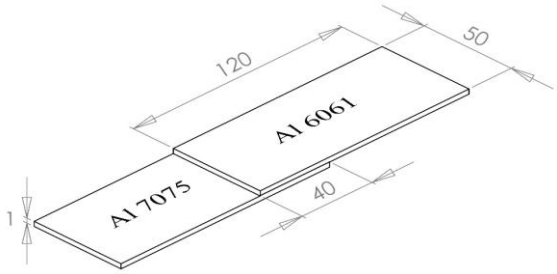

Fig.4
Dimensions of the diffusion bonded samples (millimeters).

T**able1**
Chemical composition of aluminum alloys.

Alloy	Si	Fe	Cu	Mn	Mg	Cr	Zn	Ti	V
7075	0.35	0.5	1.2	0.30	1.85	0.1	5.0	0.3	-
6061	0.63	0.17	0.32	0.52	1.08	-	-	0.02	0.01

Table 2
Important diffusion bonding process parameters.

Parameter	Level				
	-2	-1	0	+1	+2
Bonding temperature(*C*)	400	450	500	550	600
Bonding pressure(*Bar*)	20	40	60	80	100
Holding time(*min*)	30	60	90	120	150

Table 3
Experimental design matrix and results.

Expt. No.	Codec value			Orginal value			Shear strength /*Mpa*
	Bonding temperature (*C*)	Bonding pressure (*Bar*)	Holding time (*min*)	Bonding temperature (*C*)	Bonding pressure (*Bar*)	Holding time (*min*)	
1	+1	-1	+1	550	40	120	144
2	+1	+1	+1	550	80	120	163
3	-1	-1	-1	450	40	60	96
4	-1	+1	-1	450	80	60	109
5	-1	+1	+1	450	80	120	108
6	+2	0	0	600	60	90	146
7	-2	0	0	400	60	90	105
8	+1	+1	-1	550	80	60	175
9	0	0	0	500	60	90	151
10	-1	-1	0	450	40	90	124
11	0	-2	0	500	20	90	90
12	0	0	0	500	60	90	121
13	0	+2	0	500	100	90	119
14	0	0	+2	500	60	150	148
15	+1	-1	-1	550	40	60	141
16	0	0	-2	500	60	30	107

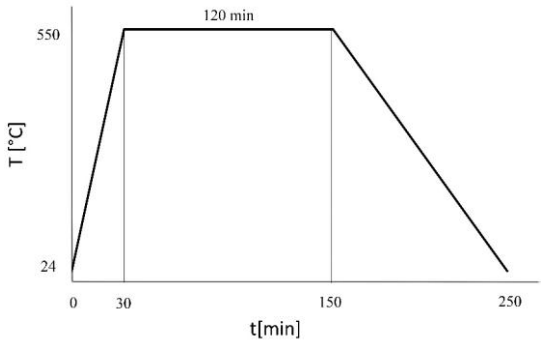

Fig.5
Connection cycle in 120 minutes (temperature,time).

2.3 Mechanical tests

The tensile test was performed by a 100-ton capacity Santam hydraulic servo unit, which was made in Iran. All tests were performed at room temperature. The loading rate in all tests is constant and equal to 0.1 *mm* / *min*. At least three samples have been tested for each condition to ensure the accuracy of the results. In each experiment, the load continues until the fragment is completely broken.

2.4 Developing empirical relationships

The response, namely shear strength (S_S) is the function of bonding temperature (T), bonding pressure (P) and holding time (t), which can be expressed as:

$$S_S = f\{T, P, t\} \tag{1}$$

The second order polynomial (regression) equation is used to represent the response surface Y. The selected polynomial could be expressed as [24]

$$Y = b_0 + b_1(T) + b_2(P) + b_3(t) + b_{11}(T^2) + b_{22}(P^2) + b_{33}(t^2) + b_{12}(TP) + b_{13}(Tt) + b_{23}(Pt) \quad (2)$$

The coefficient is obtained by applying central composite rotatable design using the Minitab statistical software package. After determining the significant coefficients (at 95% confidence level), the empirical relationships is developed using this coefficient. The final relationship is obtained to estimate shear strength. It is given as follow:

$$S_S = 147.2 + 16.75T + 6.75P + 6.75t - 4.52T^2 - 9.75P^2 - 4.02t^2 + 7.00TP \quad (3)$$

Using the empirical relationships developed above, the shear strength was estimated for different combinations of temperature, pressure and holding time.

2.5 Microscopic photographs of the fracture cross-section

Optical microscope images of the cross-section of the junction failure obtained in the optimum condition from Relation 3 using the jsm-840A microscope are shown in Figs. 6 and 7. The penetration of the layers in the surface transition zone is observed in the samples. The infiltration zone is uniform, with an average surface thickness of 10 to 15 μm. In FCC compressed crystal structures aluminum diffuses through vacancies because the drive energy required to penetrate through the vacancy in this type of network is less than other mechanisms [25]. In fact, this mechanism is the most dominant and most important intrusion mechanism in most metals. According to the images, no micro-cavities and cavities related to the Kendall effect were formed in the joint, which could be due to the nearness of the diffusion coefficients of Al 6061 and Al 7075 (about 1.89×10^{-12}) [26]and the same atomic mass of the constituent element (27 g / mol).

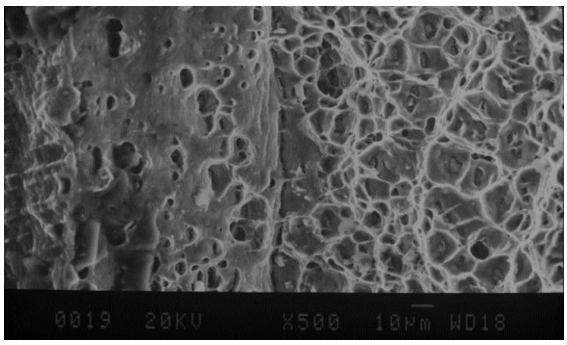

Fig.6
SEM image of cross-sectional area formed under conditions: temperature 550 ° *C*, pressure 80 *bar* and 120 *min* time with magnification of 500.

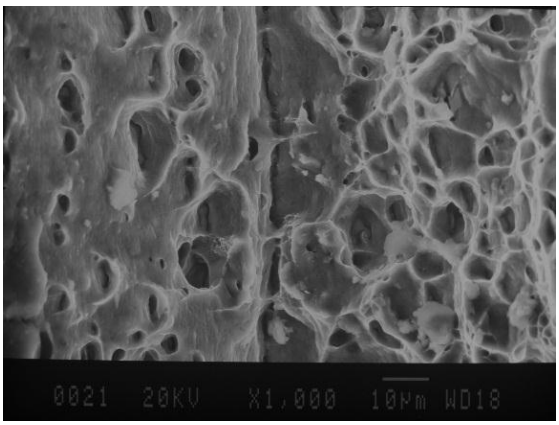

Fig.7
SEM image of cross-sectional area formed under conditions: 550 ° *C*, 80 *bar* pressure and 120 *min* time with magnification 1000.

Formation of intermetallic compounds during intrusive binding according to Filbert's theory, intermetallic compounds are formed in succession, and the second phase begins to germinate and grow only when the first phase reaches a certain thickness. In addition, the process of formation of intermetallic compounds is strongly dependent

on the thickness of the base metals [27]. The rate of formation of the new phase by intrusion in the solid state depends on the rate of diffusion and the reaction rate in the common season. The penetration rate is strongly dependent on temperature and simple kinetics rules can be used in this regard. However, other factors such as grain size, grain boundary migration, and density of dislocations can influence the penetration rate [28].

2.6 Repair cracks

In the current research, aluminum 6061 alloy was used to make the cracked piece and aluminum 7075 alloy as the patch. The size of specimen was 150×50×1 *mm*. the specimens were cut from 6061 aluminum sheets. An initial crack of 10 *mm* length and with an angle of 90 degrees relative to the loading was created in the center of the piece by laser, as shown in Fig. 8. In order to hold the specimen inside the device clips, 20 *mm* was considered on each side. The material properties and geometric parameters of the cracked plate and diffused patch are shown in Table 4.

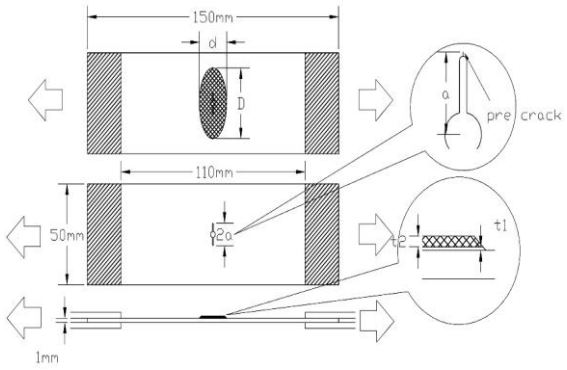

Fig.8
Specimen's details.

Table 4
Dimensions and material properties.

Layer	Made in	Length(*mm*)	Width(*mm*)	Thickness(*mm*)	Material properties
Al6061	china	150	50	1	$E = 73.01\ GPa\ ,\ \upsilon = 0.33$
Al7075	china	30	20	0.3	$E = 68.9\ GPa\ ,\ \upsilon = 0.33$

The cracked piece with 10 *mm* crack length are shown in Fig.9. Fig. 10 shows a 10 *mm* cracking piece repaired with a 3 *cm* by 2 *cm* patch. Fig. 11 shows an image of a 10 *mm* laser-generated crack with a 10x magnification. The patches with rectangular, elliptical, square and circular geometrical shapes were connected to the cracked piece using the diffusion process at optimum conditions and after performing the tensile test the maximum amount of force tolerated by the repairing piece was obtained and are shown in the various diagrams in the results section. The thickness of the patch is not studied in this study and the thickness of the patches is considered in all cases. Fig. 12 shows the growth of the crack until the fragment is completely broken.

Fig.9
Sample with 10 *mm* crack.

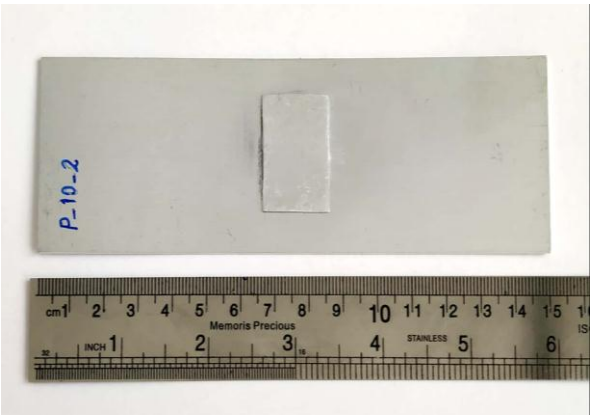

Fig.10
Specimen repaired with 10 *mm* crack.

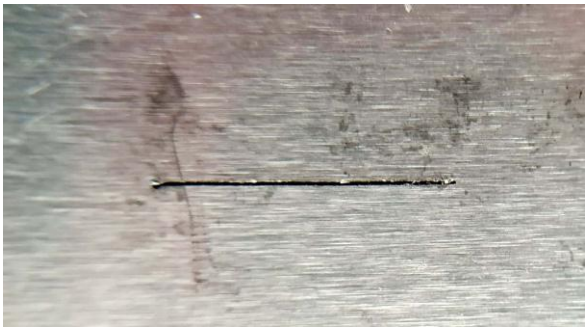

Fig.11
10 *mm* crack generated by laser with 10x magnification.

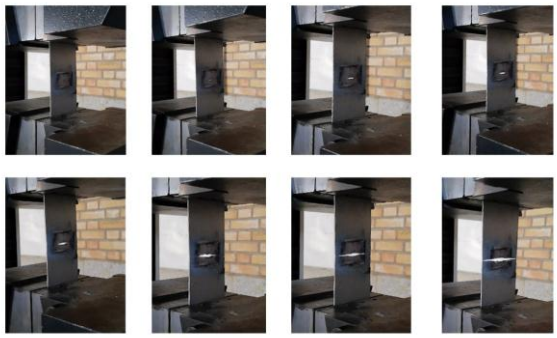

Fig.12
Crack propagation stages of repaired piece.

2.7 Numerical simulation

The extended finite element method, also known as XFEM, does not require the creation of a circular grid around the crack tip as well as the initial crack orientation and can easily be modeled by crack growth. In this method, a displacement function is defined as the combination of the displacement of nodes outside the crack zone, the nodes in which the crack is created, and the nodes around the crack tip. In this way, when a crack is created in one element, the element is divided into two parts and new nodes known as phantoms are created and two new elements are created from the first element before the crack is created. The two new elements are not interconnected at the contact site, thereby creating a modeling crack. In the new XFEM method, many of the complexities and limitations of the old methods have been eliminated by using element enrichment.

The cracked and patched plate is arranged in a square and regular with 1*mm*×1*mm* meshes of type C3D20 (Figs. 13,14). The patch is connected to the piece using a node constraint and the separation condition of this joint in the simulation process was defined as If the shear stress at each node of connection exceeds the maximum value obtained from the tests, two points would separate from each other. After several steps of modeling and comparing the responses with the experimental results, the dimensions of the elements are finer and are selected by converging the responses of the above dimensions.

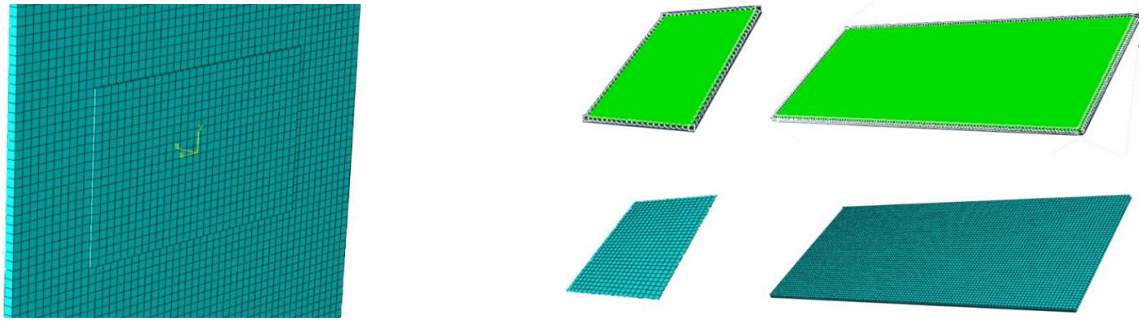

Fig.13
Finite element model of cracked panel and patch.

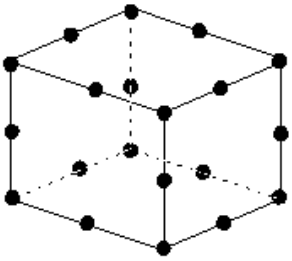

Fig.14
Quadratic element (20-node brick, C3D20).

with the finite element simulations used in Abacus software, the crack growth and contour of stress due to displacement at a rate of 0.1*mm* / *min* in the Fig.15 are shown.

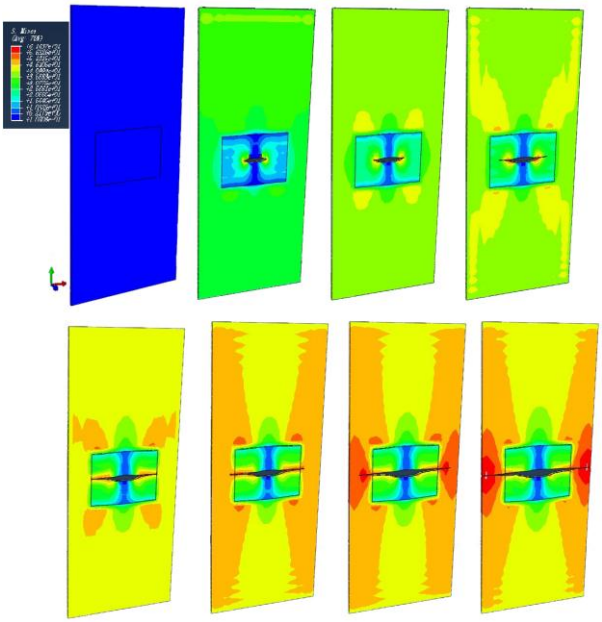

Fig.15
Crack growth and stress contour due to displacement 0.1*mm* / *min*.

3 RESULTS AND DISCUSSION

Fig. 16 is obtained from relation 3 and represents the estimated values of shear strength of diffusion bonded joints for different combinations of temperature, pressure and holding time. By examining this figure, it can be concluded that the highest amount of shear stress and thus the best joint formed in the diffusion process is in the temperature

range of 560 to 580 ° *C* and the pressure is 65 to 75 *bar* and the time is 90 to 110 minutes. And so this temperature, pressure and time range were chosen to repair the parts and attach the patch to the piece.

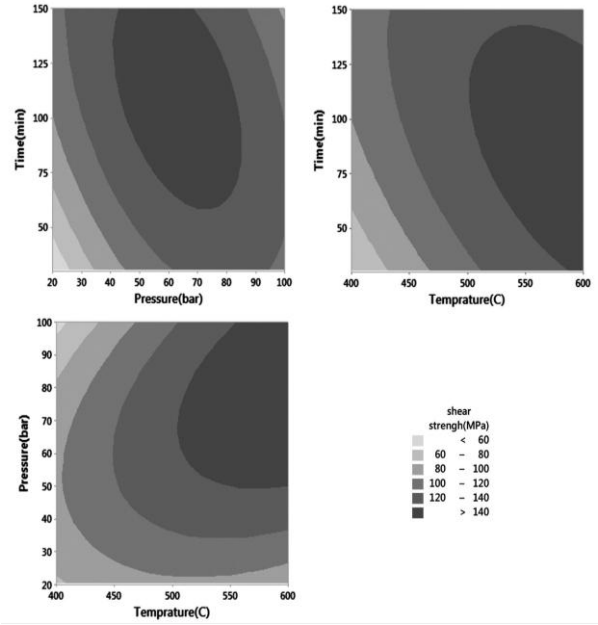

Fig.16
Contour Plots of shear strength (*Mpa*).

3.1 Rectangular patches

Fig. 17 shows the effect of the length to with ratio on the final force tolerated by the repaired piece with rectangular patch. The patch area is equal to 6 cm^2 in all ratios. Increasing the patch length in parallel with the crack leads to increased patching efficiency and as the patch length increases, the gradient of this increase decreases. As the patch width increased, the amount of final force tolerated by the piece decreased. Where *D/d* is 1, the patch is square. A square patch has a lower efficiency than a rectangular patch whose larger side is parallel to the crack and is more efficient than a rectangle whose larger side is perpendicular to the crack.

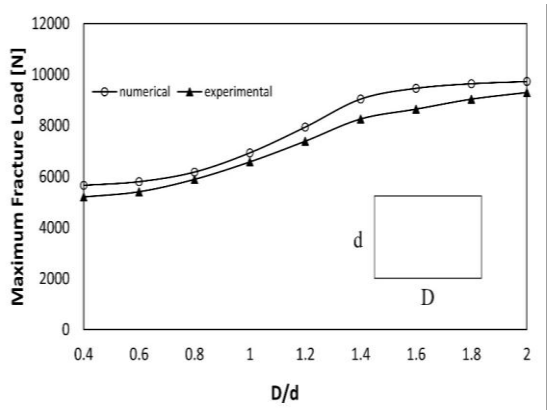

Fig.17
The effect of the length per width ratio on the final force tolerated by the repaired piece.

Fig. 18 shows the effect of the parallel length with crack of the rectangular patch on the final force tolerated by the repaired piece. It shows that the increase length of the patch in parallel with the crack leads to an increase in patch efficiency. As the patch length increases, the gradient decreases, which may indicate the optimal length for the patch. Fig. 19 shows the effect of the perpendicular length of the rectangular patch crack on the final force tolerated by the repaired piece. By increasing the length of the patch perpendicular to the patch, the final force tolerated by the segment increased with a lower inclination than the previous one. It can be concluded that increasing this side of patch has less effect on the repair efficiency and this increase may be due to the increased cross-sectional area and reduce the overall stress on the piece.

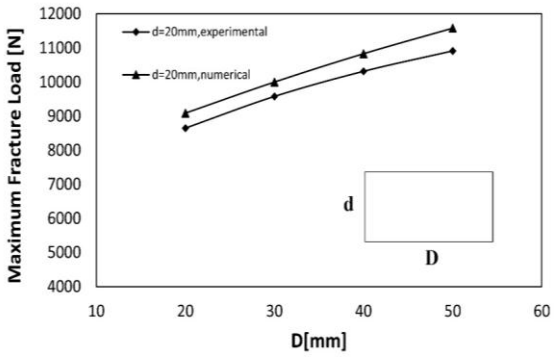

Fig.18
The effect of patch length parallel to crack line on the final force tolerated by the repaired piece.

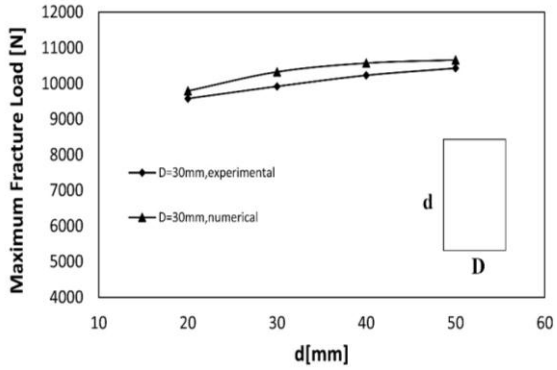

Fig.19
The effect of patch length perpendicular to crack on the final force tolerated by the repaired piece.

3.2 Square patches

Fig. 20 shows the effect of square patch dimensions on the final force tolerated by the repaired piece. As expected, with the increasing square dimensions, the amount of final force tolerated by the repaired piece increases. The magnitude of this increase is approximately between the rectangular patch perpendicular and parallel to the crack.

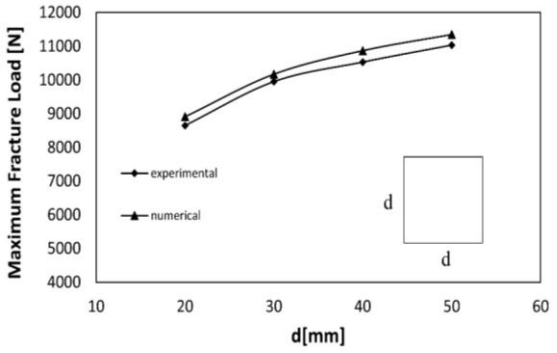

Fig.20
The effect of side length of square patch on the final force tolerated by the repaired piece.

3.3 Elliptical patches

As illustrated in Fig. 21 with constant area of elliptical patch (6 cm^2) when the ratio of parallel diameter per perpendicular diameter to crack increase that means the patch expanded in line with the crack, the maximum fracture load that repaired piece tolerate pickup. By increasing the diameter perpendicular to the crack the amount of force tolerated by the piece decreases. It seems that repairing with the elliptical patch when the major diameter is parallel to crack is more effective than that for the major diameter perpendicular to crack.

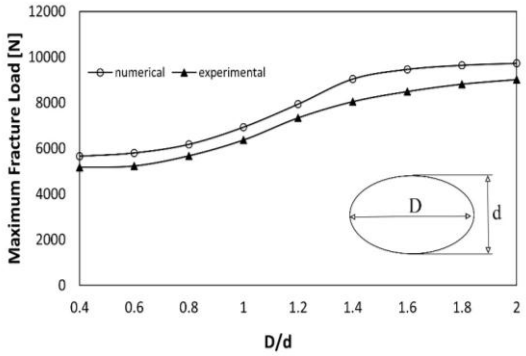

Fig.21
The effect of the major per minor ratio on the final force tolerated by the repaired piece.

Comparison between Figs. 17 and 21 shows that the overall trend of the maximum force changes in the rectangular and elliptical patch are somewhat similar. By comparing the numbers, it can be concluded that the rectangular patch is more efficient than the elliptical patch.

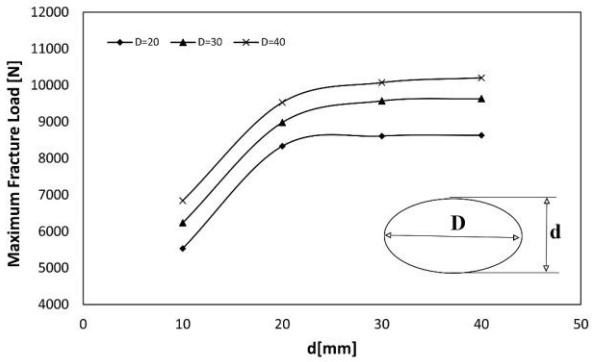

Fig.22
The effect of variation of minor axis, major axis of patch on the final force tolerated by the repaired piece.

For an elliptical patch, the variation in the final force tolerated by the repaired piece with the variation in the size of the patch is shown in Fig. 22. From Fig. 22, it is observed that for the same minor axis length, maximum fracture load increase as major axis length increases, and there exists an optimum minor axis length. Elliptical patch ($d < D$) is more effective as compared to circular patch ($D=d$). Elliptical patch ($d > D$) is less effective as compared to elliptical patch ($d < D$). It is noted that the optimum minor axis length is 33 *mm*.

3.4 Circular patches

Fig. 23 shows the effect of the diameter of the circular patch on the final force tolerated by the repaired piece. By increasing the diameter of the patch, the tolerance threshold increases. As the diameter increases, the amount of slope decreases. The amount of force tolerated per unit area in circular patches is less than the square and the rectangle parallel to the crack.

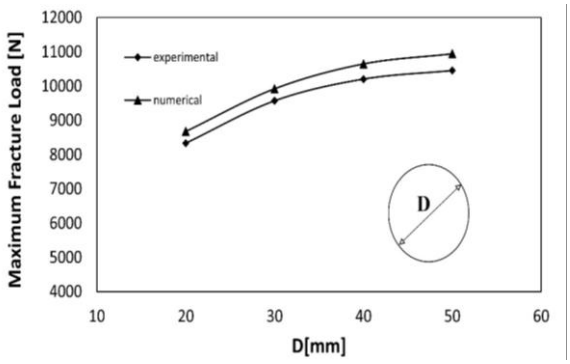

Fig.23
The effect of diameter of circular patch on the final force tolerated by the repaired piece.

4 CONCLUSIONS

In this study, the maximum amount of shear stress tolerance in lap joint made by diffusion in aluminum alloys 7075 and 6061 was determined using composite rotatable centered design in different temperature, pressure and time ranges. Then, we used these bonding conditions to repair the cracked parts with the above alloys and different patches and finally obtained the following results:

- The empirical relation was derived to predict the shear strength for diffusion bonding of aluminum alloys 7076 and 6061 in terms of parameters affecting the diffusion process, temperature, pressure and time.
- The strongest shear bonding and consequently the highest shear stress tolerated by the specimen was produced at 570 ° *C* 70 bar and 100 minutes. This may be due to the formation of optimum diffusion layer.
- The temperature, pressure and time parameters of the connection and diffusion process are not independent of each other and have the optimum value, which means that overloading each has the opposite effect and reduces the bond strength.
- The bonding temperature has the greatest impact on the final shear stress of the joint compared to pressure and time.
- Diffusion coupling is an effective way of repairing cracked parts that can provide repair with same metallic material and different metallic material patches and can eliminate disadvantages such as adhesion failure and different expansion coefficient of patch and defective part in the repair process.
- The patch shape is effective in repairing the cracked part by the diffusion process and can reduce or increase repair efficiency.

In a patch with fix area connected to the cracked part by the diffusion process, the efficiency of a rectangular patch when the length of the rectangle is parallel to the crack is higher than other shapes. Then, the ellipse patch, where the large diameter is parallel to the crack, the square, and the circle have the highest efficiency respectively. The rectangle and the ellipse have the least efficiency when the larger side and the larger diameter are perpendicular to the crack.

REFERENCES

[1] Khan M.A., Kumar S., 2017, Interfacial stresses in single-side composite patch-repairs with material tailored bondline, *Mechanics of Advanced Materials and Structures* **25**(4): 304-318.

[2] Therall E.W., 1972, Failure in Adhesively Bonded Structures, Bonded Joints and Preparatoin for Bonding, AGARD-CP-102.

[3] Baker A.A., 1984, Repair of cracked or defective metallic aircraft components with advanced fibre composites—an overview of Australian work, *Composite Structures* **2**(2): 153-181.

[4] Ghasemi F.A., Anaraki A.P., Rouzbahani A.H., 2014, Using XFEM for investigating the crack growth of cracked aluminum plates repaired with fiber metal laminate (FML) patches, *Modares Mechanical Engineering* **13**(14): 15-27.

[5] Ghasemi A.R., Mohammadi Fesharaki M., Mohandes M., 2017, Three-phase micromechanical analysis of residual stresses in reinforced fiber by carbon nanotubes, *Journal of Composite Materials* **51**(12): 1783-1794.

[6] Kurgan N., 2014, Investigation of the effect of diffusion bonding parameters on microstructure and mechanical properties of 7075 aluminium alloy, *The International Journal of Advanced Manufacturing Technology* **71**(9-12): 2115-2124.

[7] Hinotani S., Ohmori Y., 1988, The microstructure of diffusion-bonded Ti/Ni interface, *Transactions of the Japan Institute of Metals* **29**(2): 116-124.

[8] Nishi H., Araki T., Eto M., 1998, Diffusion bonding of alumina dispersion-strengthened copper to 316 stainless steel with interlayer metals, *Fusion Engineering and Design* **39**: 505-511.

[9] Yilmaz O., Aksoy M., 2002, Investigation of micro-crack occurrence conditions in diffusion bonded Cu-304 stainless steel couple, *Journal of Materials Processing Technology* **121**(1): 136-142.

[10] Yilmaz O., Celik H., 2003, Electrical and thermal properties of the interface at diffusion-bonded and soldered 304 stainless steel and copper bimetal, *Journal of Materials Processing Technology* **141**(1): 67-76.

[11] Kumar A. M., Hakeem S. A., 2000, Optimum design of symmetric composite patch repair to centre cracked metallic sheet, *Composite Structures* **49**(3): 285-292.

[12] Brighenti R., 2007, Patch repair design optimisation for fracture and fatigue improvements of cracked plates, *International Journal of Solids and Structures* **44**(3-4): 1115-1131.

[13] Okafor A.C., Singh N., Enemuoh U.E., Rao S.V., 2005, Design, analysis and performance of adhesively bonded composite patch repair of cracked aluminum aircraft panels, *Composite Structures* **71**(2): 258-270.

[14] Albedah A., Bouiadjra B. B., Mhamdia R., Benyahia F., Es-Saheb M., 2011, Comparison between double and single sided bonded composite repair with circular shape, *Materials & Design* **32**(2): 996-1000.

[15] Mahendran G., Babu S., Balasubramanian V., 2010, Analyzing the effect of diffusion bonding process parameters on bond characteristics of Mg-Al dissimilar joints, *Journal of Materials Engineering and Performance* **19**(5): 657-665.
[16] Kurt B., Orhan N., Evin E., Çalik A., 2007, Diffusion bonding between Ti–6Al–4V alloy and ferritic stainless steel, *Materials Letters* **61**(8-9): 1747-1750.
[17] Wei Y., Aiping W., Guisheng Z., Jialie R., 2008, Formation process of the bonding joint in Ti/Al diffusion bonding, *Materials Science and Engineering A* **480**(1-2): 456-463.
[18] Kenevisi M.S., Khoie S.M., 2012, A study on the effect of bonding time on the properties of Al7075 to Ti–6Al–4V diffusion bonded joint, *Materials Letters* **76**: 144-146.
[19] Chen H., Cao J., Tian X., Li R., Feng J., 2013, Low-temperature diffusion bonding of pure aluminum, *Applied Physics A* **113**(1): 101-104.
[20] Kumar S., Kumar P., Shan H.S., 2007, Effect of evaporative pattern casting process parameters on the surface roughness of Al–7% Si alloy castings, *Journal of Materials Processing Technology* **182**(1-3): 615-623.
[21] Mahendran G., Balasubramanian V., Senthilvelan T, 2009, Developing diffusion bonding windows for joining AZ31B magnesium–AA2024 aluminium alloys, *Materials & Design* **30**(4): 1240-1244.
[22] Dehghanpour S., Nezamabadi A., Attar M., Barati F., Tajdari M, 2019, Repairing cracked aluminum plates by aluminum patch using diffusion method, *Journal of Mechanical Science and Technology* **33**(10): 4735-4743.
[23] Ismail A., Hussain P., Mustapha M., Nuruddin M.F., Saat A.M., Abdullah A., Chevalier S., 2016, Fe-Al diffusion bonding: effect of reaction time on the interlayer thickness, *Journal of Mechanical Engineering* **13**(2): 10-20.
[24] Montgomery D.C., 2017, *Design and Analysis of Experiments*, John Wiley & Sons.
[25] Jafarian M., Paidar M., 2016, The comparison of microstructure and mechanical properties of diffusion joints of 5754, 6061, and 7039 aluminum alloys to AZ31 magnesium alloy, *Journal of Advanced Materials in Engineering* **35**(1): 11-21.
[26] Fernandus M.J., Senthilkumar T., Balasubramanian V., 2011, Developing temperature–time and pressure–time diagrams for diffusion bonding AZ80 magnesium and AA6061 aluminium alloys, *Materials & Design* **32**(3): 1651-1656.
[27] Fernandus M.J., Senthilkumar T., Balasubramanian V., Rajakumar S., 2012, Optimising diffusion bonding parameters to maximize the strength of AA6061 aluminium and AZ31B magnesium alloy joints, *Materials & Design* **33**: 31-41.
[28] Kundu S., Chatterjee S., 2008, Characterization of diffusion bonded joint between titanium and 304 stainless steel using a Ni interlayer, *Materials Characterization* **59**(5): 631-637.